The coherent interlayer resistance of a single, rotated interface between two stacks of AB graphite

K. M. Masum Habib,[1,a)] Somaia S. Sylvia,[1] Supeng Ge,[2] Mahesh Neupane,[1] and Roger K. Lake[1,b)]
[1]Department of Electrical Engineering, University of California, Riverside, California 92521-0204, USA
[2]Department of Physics and Astronomy, University of California, Riverside, California 92521-0204, USA

(Received 22 August 2013; accepted 17 November 2013; published online 13 December 2013)

The coherent, interlayer resistance of a misoriented, rotated interface between two stacks of AB graphite is determined for a variety of misorientation angles. The quantum-resistance of the ideal AB stack is on the order of 1 to 10 $m\Omega\,\mu m^2$. For small rotation angles, the coherent interlayer resistance exponentially approaches the ideal quantum resistance at energies away from the charge neutrality point. Over a range of intermediate angles, the resistance increases exponentially with cell size for minimum size unit cells. Larger cell sizes, of similar angles, may not follow this trend. The energy dependence of the interlayer transmission is described. © *2013 AIP Publishing LLC*. [http://dx.doi.org/10.1063/1.4841415]

There is rapidly growing interest in vertically stacked van der Waals materials for electronic device applications.[1–7] In such structures, the interfaces between different materials will, in general, be misoriented with respect to each other.[8] THz cutoff frequencies have been predicted for such devices.[6] At such high frequencies, any small series resistance can degrade performance. For example, an emitter contact resistance of 2.5 $\Omega\,\mu m^2$ is required to achieve a THz cutoff frequency in a heterostructure bipolar transistor.[9] Understanding the effect of the misorientation on the interlayer resistance is required to fully understand the design requirements and performance of proposed vertically stacked devices.

The most well studied and well understood of the van der Waals material are graphite and graphene.[8,10–13] There is a long history of investigations of the *c*-axis resistance of graphite.[11,12,14–17] This body of work focused on stacks of kish graphite or highly ordered pyrolytic graphite with a random ensemble of stacking faults in the diffusive limit.

The effect of misorientation on the electronic structure of bilayer graphene has been studied extensively both theoretically and experimentally.[18–27] After a few degrees misorientation, the in-plane dispersion becomes linear, and after about 10° misorientation, the in-plane velocity is the same as that of single-layer graphene. Thus, the two misoriented layers of graphene act as if they are electronically decoupled.

The interlayer resistance of misoriented bilayer graphene has received less attention.[28–30] The calculated coherent interlayer resistance as a function of rotation angle θ is found to vary by 16 orders of magnitude as the misorientation angle changes from 0° to 30°.[28] The values vary from approximately $10^{15}\,\Omega\,\mu m^2$ to $0.1\,\Omega\,\mu m^2$. The room-temperature, phonon-mediated interlayer resistance of misoriented bilayer graphene shows far less dependence on the misorientation angle.[29,30] It changes by less than an order of magnitude as the angle varies from 0° to 30°.[29,30] Its calculated value is approximately $100\,\Omega\,\mu m^2$ over a range of intermediate rotation angles.[29] Experimental measurements found approximately an order of magnitude larger resistance that varied from $750\,\Omega\,\mu m^2$ to $3400\,\Omega\,\mu m^2$ as the angle varied from 5° to 24°.[30,31] Calculations of the interlayer magnetoresistance of misoriented bilayer graphene ribbons show a large magnetoresistance ratio accompanied by large transmission peaks or Fano resonances resulting from edge states.[32]

In this work, we calculate the transmission through two stacks of AB graphite that are rotated with respect to each other at their interface. In such a structure, the semi-infinite AB graphite stacks act as ideal leads so that injection is well defined using the usual non-equilibrium Green function (NEGF) approach. The resistance can be calculated for $\theta = 0°$ providing a minimum baseline value. This type of structure is consistent with the proposed vertically stacked van der Waals structures. We determine the coherent, interlayer resistance for a wide range of rotation angles. The energy dependence of the coherent interlayer resistance is calculated and discussed.

The twisted bilayer graphene (TBG) supercell (i.e., the primitive cell of the commensurate twisted bilayer) is created following the method described in Ref. 23. The top layer of the TBG supercell is used to create an AB stacked bilayer graphene supercell which, in turn, is used to create the top contact. Similarly, the bottom contact is created using the bottom layer of the TBG supercell. Thus, the twisted structure consists of two AB oriented stacks that are rotated with respect to each other as shown in Fig. 1.

The interlayer coherent transport through the twisted structure is modeled using the NEGF formalism with an empirical tight binding Hamiltonian. The coherent resistance is calculated using

$$R = 1 \Big/ \left[2\frac{e^2}{\hbar} \int \frac{dE}{2\pi}\, T(E) \left(-\frac{\partial f}{\partial E} \right) \right], \tag{1}$$

where $f(E)$ is the Fermi function. The transmission $T(E)$ is given by $T(E) = \int_{1^{st}BZ} d\mathbf{k}\ T(E, \mathbf{k})$, where $\mathbf{k}$ is 2D wave vector in the TBG Brillouin zone and $T(E, \mathbf{k})$ is the wavevector

a)Email: khabib@ee.ucr.edu
b)Email: rlake@ee.ucr.edu

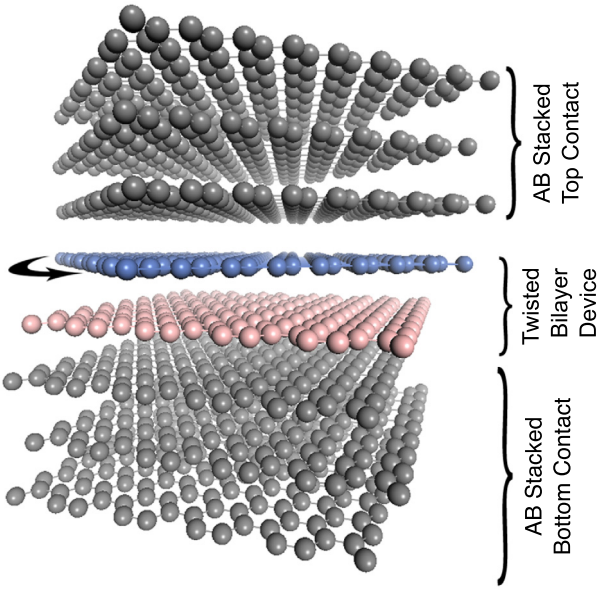

FIG. 1. Atomistic geometry of the rotated interface. It consists of two AB oriented stacks that are rotated with respect to each other. The interface layers where the misorientation occurs have been colored for visualization. The two misoriented layers are the "device" in the NEGF calculation.

resolved transmission calculated using NEGF. A tight-binding Hamiltonian is used. The in-plane nearest neighbor hopping element is $t = 3.16\,\text{eV}$.[13] The model developed by Perebeinos *et al.* is used for the out-of-plane coupling.[29] Details of the methods are given in the supplementary material.[33]

Figs. 2(a) and 2(b) show the zero-temperature, interlayer resistance over a range of Fermi energies from ± 1 eV around the charge neutrality point in Fig. 2(a) and from ± 0.7 eV in Fig. 2(b) for a range of rotation angles from 0° to 27.79°. The lowest curve is the coherent resistance of the ideal AB stack with $\theta = 0°$. This resistance is the fundamental limiting "quantum resistance" inversely proportional to the number of transverse modes available to carry the current at a given energy. This quantity has recently been calculated for other materials to determine the fundamental lower limit on the contact resistance.[34]

The magnitude of the coherent interlayer resistance increases several orders of magnitude as the layers become misaligned. The legends in Figs. 2(a) and 2(b) are ordered according to the size of the corresponding commensurate unit cell so that, among the rotated interfaces, $\theta = 21.8°$ gives the smallest unit cell and $\theta = 2.87°$ gives the largest unit cell. For angles >7.34°, the magnitude of the resistance increases with the size of the unit cell. This is the same trend found for the coherent, interlayer resistance of bilayer graphene discussed in Ref. 29. The resistances for angles $\leq 7.34°$, fall off rapidly as the energy moves away from the charge neutrality point, so that at larger energies, this trend fails for the smaller rotation angles.

All of the angles shown *except* 20.31° fall along the line of minimum unit-cell size shown in Fig. 2 of Ref. 23. A 1°–2° change in the rotation angle can change the commensurate unit cell size by over 3 orders of magnitude. Thus, it is interesting to consider two very close angles with a large difference in cell size. Two such angles are 21.78° in Fig. 2(a) and 20.31° in Fig. 2(b). These two angles differ by 1.47°, yet the 21.78° rotation gives the smallest unit cell with a lattice constant of 6.51 Å, and the 20.31° rotation gives the second largest unit cell with a lattice constant of 36.23 Å. Near the charge neutrality point, the resistance of the 20.31° structure is the highest of all of the structures. This follows the trend of increasing resistance with unit cell size. At energies ± 0.2 eV away from the charge neutrality point, the resistance rapidly falls 4 to 5 orders of magnitude and approaches

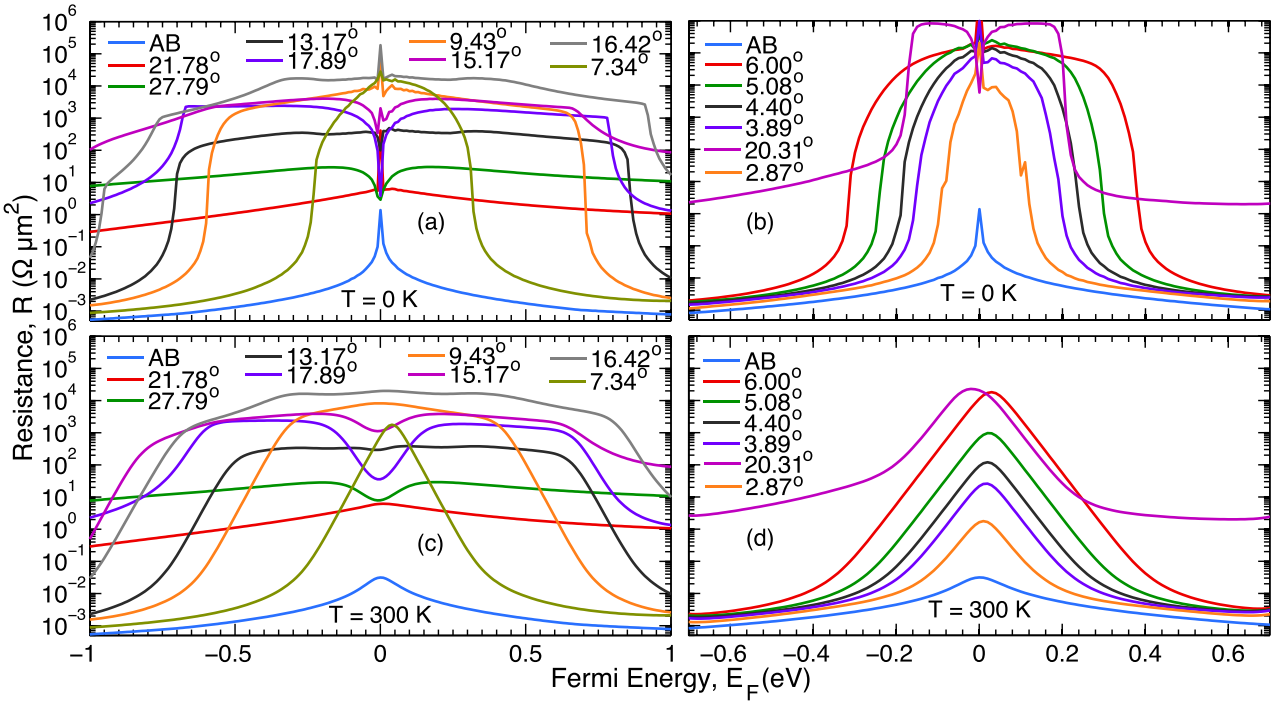

FIG. 2. (a, b) Zero temperature coherent contact resistance of twisted bilayer graphene as a function of Fermi Energy for different rotation angles. (c, d) Room temperature coherent contact resistance of twisted bilayer graphene as a function of Fermi energy for different rotation angles.

the resistance of the 21.78° structure. This can be understood by considering the extended zone scheme of the reciprocal lattice. At this energy, the Fermi surfaces around the K points that coincide in the extended zone scheme of the 21.78° structure just begin to touch.

We refer to the magnitude of the K points of the 21.78° structure in the extended zone scheme as K_2. They are illustrated in Fig. 3. They lie in the second Brillouin zones and their magnitude is $K_2 = \sqrt{7}K_0$, where K_0 is the magnitude of the K point in the first Brillouin zone, $K_0 = \frac{4\pi}{3a}$, and $a = 2.46$ Å. At a rotation angle of 20.31°, these points are misaligned by $\delta\theta = 1.47°$, and their centers are misaligned in k-space by $\delta k = \sqrt{7}K_0\delta\theta = 0.116$ Å^{-1}. The radius (k_r) of the Fermi circle in the $k_x - k_y$ plane of ideal AB graphite at $E = 0.2$ eV is $k_r = 0.058$ Å$^{-1} = \delta k/2$. Thus, at $E = 0.2$ eV in the 20.31° structure, the Fermi surfaces begin to touch around the K_2 points. In the extended zone scheme, at low energies, in the 20.31° structure, conduction takes place at K points with a magnitude of $\sqrt{217}K_0$. At $E = 0.2$ eV, conduction begins at the K_2 points with a magnitude of $\sqrt{7}K_0$. Since the matrix element coupling the states decays exponentially with the magnitude of k, there is a sudden decrease in resistance when a channel opens at a much smaller k-point in the extended zone.[28]

As the magnitude of the energy increases, new channels open around K-points in the extended zone. When these K points are closer to Γ, the resistance suddenly drops and approaches a new value dominated by the transmission through the smaller K points. For example, at ~0.8 eV, the $\theta = 17.89°$ structure begins to conduct around the K_2 points and its resistance falls several orders of magnitude to that of the $\theta = 21.78°$ structure. When the resistance falls to the same order of magnitude as that of the ideal AB structure, it indicates that the transmission is taking place around the K-points of the first Brillouin zone. At higher energies, this is the dominant transport channel for all of the low-angle structures as can be seen in Fig. 2(b).

When a new channel opens up in the extended zone scheme, it will generally appear in the reduced zone of the commensurate primitive cell as a sudden movement of the transmission in k-space. This results from the fact that new K points in the extended zone do not, in general, map onto the K points of the reduced Brillouin zone. For the 20.31° structure, the transmission in the reduced Brillouin zone shifts from the K point to the M point at $E = 0.2$ eV.

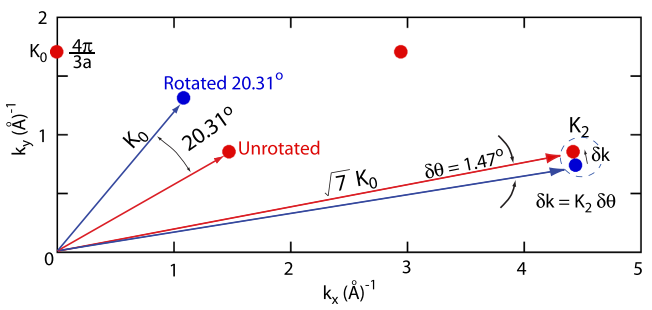

FIG. 3. Upper right quadrant of the extended Brillouin zone. The unrotated K-points are red, and the rotated K-points are blue. The rotation angle is 20.31°. In the second Brillouin zone, at a distance $\sqrt{7}K_0$ from Γ, the K-points of the unrotated and rotated lattices are misaligned by 1.47°. At low energies, transmission takes place around a K point with magnitude $\sqrt{217}K_0$. At 0.2 eV, transmission begins around the K-point at $\sqrt{7}K_0$.

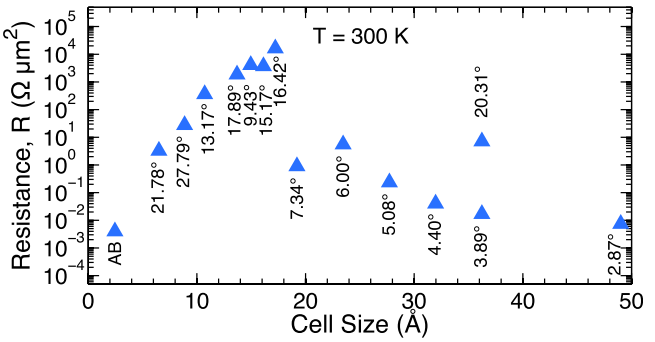

FIG. 4. Room temperature coherent (R_c) resistance as a function of the commensurate unit cell size at $E_F = 0.26$ eV. The corresponding angles are shown in the figure.

The coherent interlayer resistances at $T = 300$ K are shown in Figs. 2(c) and 2(d). They are obtained by convolving the transmission with the room temperature thermal broadening function in Eq. (1), which removes the sharpest features from Figs. 2(a) and 2(b). At room temperature, the interlayer resistances for angles ≤ 7.34° exponentially decay with energy towards the ideal unrotated value.

The room temperature resistance values for all structures are plotted in Fig. 4 at a Fermi energy of 0.26 eV as considered in Refs. 28 and 29 for rotated bilayer graphene. The values are also listed in Table I. The trend of exponentially increasing resistance with unit-cell size is clear for rotation angles ≥ 9.34°. An abrupt, three order of magnitude discontinuity in the trend occurs between 9.43° and 7.34° for the low rotation angles. In these structures, transmission is taking place around the K-points of the first Brillouin zone.

There is also the one outlying point from the 20.31° structure. While its unit-cell size is huge, and it is not a small angle, its resistance is far off of the initial trend. It has the same resistance as the smallest 21.78° structure. That is because, at an energy of 0.26 eV, its transmission is taking place around the same K points in the extended zone as that of the 21.78° structure.

TABLE I. Coherent resistance R_c, as a function of rotation angle and primitive-cell lattice constant. Resistance units are ($\Omega\,\mu$m^2). Angles are in degrees and the lattice constants are in Å. $T = 300$ K and $E_F = 0.26$ eV. The angles are ordered according to the supercell size from smallest to largest.

Rotation angle θ	Lattice constant	No. of atoms	R_c
AB	2.46	2	3.89×10^{-3}
21.78	6.51	28	3.28
27.79	8.87	52	27.7
13.17	10.72	76	363
17.89	13.69	124	1860
9.43	14.96	148	4080
15.17	16.13	172	3720
16.42	17.22	196	16400
7.34	19.21	244	0.90
6.00	23.46	364	5.55
5.08	27.71	508	0.24
4.40	31.97	676	4.03×10^{-2}
3.89	36.23	868	1.69×10^{-2}
20.31	36.23	868	7.11
2.87	49.01	1588	7.45×10^{-3}

The vast number of huge commensurate primitive cells a small rotation angle away from much smaller primitive cells, as shown in Fig. 2 of Ref. 23, will not follow the exponential trend of resistance versus cell size at any energy a few hundred meV away from the charge neutrality point. Instead, their finite Fermi surfaces will overlap at some much reduced K point in the extended zone, and those K-points, corresponding to a much smaller cell size, will control the conductance.

In conclusion, the quantum-resistance of ideal AB graphene is on the order of $10^{-3} - 10^{-2}\,\Omega\,\mu\text{m}^2$. For small misorientation angles, the coherent interlayer resistance exponentially decreases towards the ideal, unrotated AB value at higher energies. For intermediate angles of minimal cell sizes, the coherent interlayer resistance exponentially increases with cell size. For intermediate angles with very large cell sizes, the resistance will correspond to a much smaller cell size of a nearby angle for any finite Fermi energy of a few hundred meV.

This work was supported in part by FAME, one of six centers of STARnet, a Semiconductor Research Corporation program sponsored by MARCO and DARPA.

[1]L. Britnell, R. V. Gorbachev, R. Jalil, B. D. Belle, F. Schedin, A. Mishchenko, T. Georgiou, M. I. Katsnelson, L. Eaves, S. V. Morozov, N. M. R. Peres, J. Leist, A. K. Geim, K. S. Novoselov, and L. A. Ponomarenko, Science **335**, 947 (2012).
[2]H. Yang, J. Heo, S. Park, H. J. Song, D. H. Seo, K.-E. Byun, P. Kim, I. Yoo, H.-J. Chung, and K. Kim, Science **336**, 1140 (2012).
[3]S. Chuang, R. Kapadia, H. Fang, T. C. Chang, W.-C. Yen, Y.-L. Chueh, and A. Javey, Appl. Phys. Lett. **102**, 242101 (2013).
[4]T. Georgiou, R. Jalil, B. D. Belle, L. Britnell, R. V. Gorbachev, S. V. Morozov, Y.-J. Kim, A. Gholinia, S. J. Haigh, O. Makarovsky, L. Eaves, L. A. Ponomarenko, A. K. Geim, K. S. Novoselov, and A. Mishchenko, Nat. Nanotechnol. **8**, 100 (2012).
[5]W. J. Yu, Z. Li, H. Zhou, Y. Chen, Y. Wang, Y. Huang, and X. Duan, Nature Mater. **12**, 246 (2013).
[6]W. Mehr, J. Dabrowski, J. Christoph Scheytt, G. Lippert, Y.-H. Xie, M. C. Lemme, M. Ostling, and G. Lupina, IEEE Electron Device Lett. **33**, 691 (2012).
[7]D. Jena, Proc. IEEE **101**, 1585 (2013).
[8]A. K. Geim and I. V. Grigorieva, Nature **499**, 419 (2013).
[9]M. J. W. Rodwell, M. Le, and B. Brar, Proc. IEEE **96**, 271 (2008).
[10]G. J. Morgan and C. Uher, Philos. Mag. B **44**, 427 (1981).
[11]D. Z. Tsang and M. S. Dresselhaus, Carbon **14**, 43 (1976).
[12]S. Ono, J. Phys. Soc. Jpn. **40**, 498 (1976).
[13]A. H. Castro Neto, F. Guinea, N. M. R. Peres, K. S. Novoselov, and A. K. Geim, Rev. Mod. Phys. **81**, 109 (2009).
[14]W. Primak and L. H. Fuchs, Phys. Rev. **95**, 22 (1954).
[15]T. Tsuzuku, Carbon **21**, 415 (1983).
[16]K. Matsubara, K. Sugihara, and T. Tsuzuku, Phys. Rev. B **41**, 969 (1990).
[17]G. Venugopal, G. S. Kim, and S.-J. Kim, Jpn. J. Appl. Phys., Part 1 **50**, 06GE06 (2011).
[18]J. M. B. Lopes dos Santos, N. M. R. Peres, and A. H. Castro Neto, Phys. Rev. Lett. **99**, 256802 (2007).
[19]X. Wu, X. Li, Z. Song, C. Berger, and W. A. de Heer, Phys. Rev. Lett. **98**, 136801 (2007).
[20]S. Latil, V. Meunier, and L. Henrard, Phys. Rev. B **76**, 201402 (2007).
[21]J. Hass, F. Varchon, J. Millán-Otoya, M. Sprinkle, N. Sharma, W. de Heer, C. Berger, P. First, L. Magaud, and E. Conrad, Phys. Rev. Lett. **100**, 125504 (2008).
[22]S. Shallcross, S. Sharma, and O. A. Pankratov, Phys. Rev. Lett. **101**, 056803 (2008).
[23]S. Shallcross, S. Sharma, E. Kandelaki, and O. A. Pankratov, Phys. Rev. B **81**, 165105 (2010).
[24]G. Trambly de Laissardiere, D. Mayou, and L. Magaud, Nano Lett. **10**, 804 (2010).
[25]A. Luican, G. Li, A. Reina, J. Kong, R. R. Nair, K. S. Novoselov, A. K. Geim, and E. Y. Andrei, Phys. Rev. Lett. **106**, 126802 (2011).
[26]J. M. B. Lopes dos Santos, N. M. R. Peres, and A. H. Castro Neto, Phys. Rev. B **86**, 155449 (2012).
[27]S. Shallcross, S. Sharma, and O. Pankratov, Phys. Rev. B **87**, 245403 (2013).
[28]R. Bistritzer and A. H. MacDonald, Phys. Rev. B **81**, 245412 (2010).
[29]V. Perebeinos, J. Tersoff, and P. Avouris, Phys. Rev. Lett. **109**, 236604 (2012).
[30]Y. Kim, H. Yun, S.-G. Nam, M. Son, D. S. Lee, D. C. Kim, S. Seo, H. C. Choi, H.-J. Lee, S. W. Lee, and J. S. Kim, Phys. Rev. Lett. **110**, 096602 (2013).
[31]The resistance values in Ωcm given by Kim *et al*. are converted to $\Omega\,\mu\text{m}^2$ using an interlayer distance of 3.4 Å so that $1\,\Omega\,\text{cm} = 3.4\,\Omega\,\mu\text{m}^2$.
[32]S. Ahsan, K. M. Masum Habib, M. R. Neupane, and R. K. Lake, J. Appl. Phys. **114**, 183711 (2013).
[33]See supplementary material at http://dx.doi.org/10.1063/1.4841415 for more detailed calculation methods.
[34]J. Maassen, C. Jeong, A. Baraskar, M. Rodwell, and M. Lundstrom, Appl. Phys. Lett. **102**, 111605 (2013).